

Improving state estimation through projection post-processing for activity recognition in football

Michał Ciszewski*, Jakob Söhl, Geurt Jongbloed

Applied Mathematics, Faculty of Electrical Engineering,
Mathematics & Computer Science, Delft University of Technology,
Delft, The Netherlands

Abstract

The past decade has seen an increased interest in human activity recognition. Most commonly, the raw data coming from sensors attached to body parts are unannotated, which creates a need for fast labelling method. Part of the procedure is choosing or designing an appropriate performance measure. We propose a new performance measure, the Locally Time-Shifted Measure, which addresses the issue of timing uncertainty of state transitions in the classification result. Our main contribution is a novel post-processing method for binary activity recognition. It improves the accuracy of the classification methods, by correcting for unrealistically short activities in the estimate.

keywords: activity recognition, wearable sensors, post-processing, performance measures

1 Introduction

In almost all areas of science and technology sensors are becoming more and more prevalent. In recent years we have seen applications of sensor technology in fields as diverse as energy saving in smart home environments [1], performance assessment in archery [2], activity monitoring of elderly [3], recognition of human stress [4], detection of mooring ships [5], early detection of Alzheimer disease [6], dietary monitoring [7] and recognition of emotional states [8], to name just a few.

Our main interest lies in the detection of human activities using sensors attached to the body. Sensors generate raw data without annotations suggesting the use of unsupervised learning methods. If a pattern specified in advance is of interest, then supervised learning and labelled data are required. However,

*Corresponding author: M.G.Ciszewski@tudelft.nl

the task of labelling activities manually from sensor data is labour-intensive and prone to error, which creates the need for fast and accurate automated methods. Human activity recognition (HAR) attracted much attention since its inception in the '90s. A plethora of methods are being used [9], with various deep learning techniques leading the charge [10, 11]. The goal of HAR is to find a sequence of activities performed by a person based on observed data. Data can come from different sources. Many researchers [12, 13, 14] use only sensors embedded in a smartphone to classify user activities. Radio-based activity recognition is less popular, but provides lower power consumption and lower cost of production of the sensors [15]. Physical sensors, such as accelerometer or gyroscope attached directly to a body or video recordings from a camera, are the most popular sources of data for activity recognition. Placement of the sensors on the body differs based on the research topic. In some cases more than one accelerometer or gyroscope is used [16, 17], but most commonly only one sensor is attached to a body [18]. Similarly, cameras can be either placed on the subject [19, 20, 21] or they can observe the subject [22, 23, 24]. Rarely, both camera and inertial sensor data is captured at the same time [25].

In case of multiple wearable sensors attached to different body parts, data are highly time-dependent and effective estimation should take into account the temporal structure of the time series. This leads to many challenges; to account for time dependencies mainstream classification techniques will need to be augmented. Alternatively, more complicated and more difficult to train methods have to be deployed. Another challenge lies in the reliability of manual labelling (in case of supervised learning). Quite often it is unreasonable to assume that labels annotating the observed data are exact with regards to timings of transitions from one activity to another [26]. Timing uncertainty can be caused by a deficiency of the manual labelling or the inability to objectively detect boundaries between different activities. This issue is well-known in the literature, for instance, Yeh et al. [27] introduced a scalable, parameter-free and domain-agnostic algorithm that deals with this problem in the case of one-dimensional time series.

In order to provide more context, we describe the dataset used for the evaluation of the methods that will be introduced later. Eleven amateur football players participated in a coordinated experiment at a training facility of the Royal Dutch Football Association of The Netherlands. Five Inertial Measurement Units (IMUs) were attached to both their shanks, thighs of both legs and pelvis. Every IMU measures six features in time: magnitude and direction of acceleration in 3 dimensions (using a 3-axis accelerometer) and magnitude and direction of angular velocity in 3 dimensions (using a 3-axis gyroscope). Athletes were asked to perform exercises on command, e.g. 'jog for 10 meters' or 'long pass'. For each athlete and exercise this resulted in a 30-dimensional time series (5 body parts times 6 features per IMU) of length varying from 4 to 14 seconds. Each athlete performed 70-100 exercises which amounts to nearly 900 time series (each with a sampling frequency of 500 Hz). Time series are labelled with the command given to an athlete, but there are still other activities performed in each of the time series, for example standing still. This causes a problem;

ignoring standing periods and treating them as part of the main signal pollutes the data and lowers the quality of the classification. Our goal is to sift through the time series for the activity of interest and to identify all time points as either standing or the other activity. Wilmes et al. [28] describe the experiment more closely.

For the remainder of this paper, following naming convention will be used. We are given a multivariate time series and an associated with it univariate time series of states. In our context, a *state* corresponds to specific human activity. Any sequence of states will be called a *state sequence*. A *label* is a state at a given time point in a state sequence. If a state sequence corresponds to the true underlying sequence of activities in a time series, then it will be called the *true labels* or the *ground truth labels*. An estimate of the true labels will be called the *estimated labels*. Specific to binary classification the term *event* refers to a time interval, in which a state sequence takes value 1, while the label directly preceding and following this time interval is not 1.

To compare the quality of competing activity recognition methods, an appropriate performance evaluation metric has to be chosen. Commonly used criteria are accuracy, precision and the *F*-measure [9, 29]. Another approach is to use similarity measures for time series classification [30], such as Dynamic Time Warping or Minimum Jump Costs Dissimilarity. Our objective is to find a performance measure that satisfies problem-specific conditions, which usually are not addressed by standard performance measures. In our case, already mentioned timing uncertainty in true labels as well as *event fragmentation* and *merging* are the problems of interest. Event fragmentation occurs when an event in true labels is represented by more than one event in estimated labels, whereas merging refers to several true events being represented by a single event in estimated labels. Ward et al. [31] provide an excellent overview of different performance metrics used in activity recognition proposing a solution to the problem of timing uncertainty as well as event fragmentation and merging. The issues mentioned above are also addressed here, however, in a different way. Our main focus regarding the performance measure for our application is on detecting time shifts in the estimated labels (which address the problem of timing uncertainty), while the fragmented or merged events influence the performance of a classifier through the number of state transitions present in the estimated labels.

The second contribution of this paper is the introduction of a post-processing procedure, which projects a binary state sequence onto a certain subset. This subset of state sequences is characterized by a condition that bounds the state durations from below. It allows us to mitigate the problem of event fragmentation in cases where some domain-specific information about state durations is available. Based on empirical evidence, the performance (as measured by standard performance measures or the one newly introduced here) of classical machine learning classifiers improves significantly by projecting the state sequence. This enables simple and fast but less accurate classification methods to be upgraded to accurate and fast classifiers.

The outline of the paper is as follows. Section 2 introduces specialized perfor-

mance measures for assessing the quality of classification in general and activity recognition in particular. Section 3 provides a method for improving any binary classification with a post-processing scheme that uses background knowledge in the specific context. In particular, it validates the state durations and provides an improved classification that satisfies the physical constraints on the state durations imposed by the context. Section 4 presents an application of the techniques in the setting of the football exercises just described.

2 Incorporating domain knowledge into the performance measure of classification

2.1 Problem-specific requirements on the performance measure

In order to choose an appropriate performance measure for a given classification task, it is important to understand the problem-specific demands on the result. Just choosing the simplest or the most common performance measure can easily lead to results that do not truthfully represent the classifiers' performance as valued by the users. In this section, we aim to highlight the main characteristics of the classification of movements based on wearable sensors and to translate them into specific requirements on the performance measure.

First, physical restrictions need to be taken into account. States that are considered in our application represent human activities. As such they cannot be arbitrarily short; there is a lower bound on the duration of these states. Hence, estimated labels that violate this lower bound indicate a bad performance. The lower bound condition requires two parameters: the lower bound and the penalty for each violation. The lower bound can either be estimated or determined by domain knowledge, while the penalty can be chosen more freely.

Second, the issue of timing uncertainty should also be addressed when designing the performance measure. To illustrate its importance more clearly, we present an example. Five people were asked to detect boundaries between activities in different time series using a visualization tool. The tool outputs an animated stick figure model¹ given sensor data.

Three time series were selected, each with one activity: running, jumping and ball kick. Respectively, the start and the end of each activity were recorded by participants. Table 1 presents the results of the experiment.

The experiment indicates there is indeed uncertainty regarding the state transitions. Granted that the sample size is very small, we notice more variation in results referring to the end of activities rather than the beginnings. Additionally, we see more variation in the results for the kick than the jumping. So the boundaries of some activities seem to be more difficult to identify than others.

¹A symbolic representation of the human body using only lines

Partic.	Running		Jumping		Kick	
	Start	End	Start	End	Start	End
P1	2	7.3	2.7	5.2	2.5	3.5
P2	2	7.5	2.7	5.2	2.5	3.9
P3	2.3	6.6	2.7	5.1	2.7	3.6
P4	2.3	7.2	2.7	5.3	2.5	4.3
P5	2.2	7.2	2.9	5.4	2.5	4.1
Avg.	2.16	7.16	2.74	5.24	2.54	3.88
Std	0.15	0.34	0.09	0.11	0.09	0.33

Table 1: The results of the labelling experiment; all times are in seconds. The two last rows show the average and the sample standard deviation for each boundary

In this section we have shown two issues that should drive the design of the performance measure. Physical restrictions, such as a lower bound on the duration of the activities, should be taken into account to prevent unrealistic classifications from being considered good estimates. Timing uncertainty should also be addressed as often the ground truth labels might not be 100% accurate.

2.2 Globally Time-Shifted distance

We define a class of Globally Time-Shifted distances (GTS distances), loosely inspired by the Skorokhod distance on the space of càdlàg functions [32, pp. 121]. Consider the set of states $\mathcal{S} = \{s_1, \dots, s_m\}$ and a metric d on \mathcal{S} . If $d(s_i, s_j) = 1 - \delta_{ij}$ for all $i, j = 1, \dots, m$, where δ_{ij} is the Kronecker delta equal to 1 if $i = j$ and otherwise 0, then d will be called the *discrete metric* on \mathcal{S} . Figure 1 shows the metric space of states in the form of weighted graph.

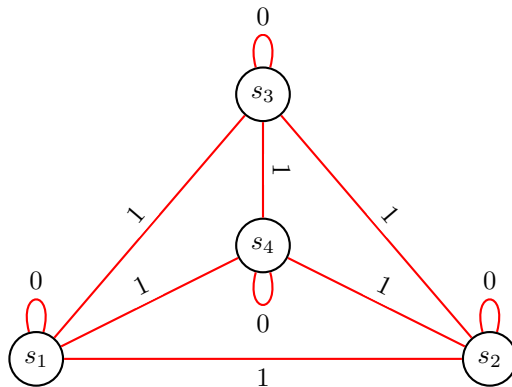


Figure 1: The graph of 4 states equipped with the discrete metric

We choose to represent state sequences using functions of time. In reality we are only able to obtain a discrete-time signal, however, the relevant information contained in such a signal is a list of all the state transitions, which can more easily be encoded in a function with continuous argument. Hence we define \mathcal{T} , the set of all càdlàg functions $f : \mathbb{R} \rightarrow \mathcal{S}$ with a finite number of discontinuities. We identify functions that are equal almost everywhere with respect to Lebesgue measure on \mathbb{R} . We define the *standard distance* between two trajectories

$$\text{dist} : \mathcal{T} \times \mathcal{T} \ni (f, g) \rightarrow \text{dist}(f, g) = \int_{\mathbb{R}} d(f(t), g(t)) dt. \quad (1)$$

If d is a metric on \mathcal{S} , then it can be shown that dist is a metric on \mathcal{T} . If d is the discrete metric on \mathcal{S} , then dist is the time spent by f in a state different than g .

The distance dist is an unsatisfying measure to compare two trajectories, since it does not incorporate the requirements posed in the previous section. In order to improve it, we start by modelling the timing uncertainty. Let $f \in \mathcal{T}$ be the ground truth state process and let f have n discontinuities j_1, \dots, j_n . The locations of the discontinuities are corrupted by additive noise:

$$j_i = J_i + X_i,$$

for all $i = 1, \dots, n$, where J_i is the true and unknown location of the i -th jump. In general, X_1, \dots, X_n are i.i.d. random variables, but in this section we will assume that $X_1 = X_2 = \dots = X_n$ (all jumps are moved by the same value; the global time shift).

We proceed to define the Globally Time-Shifted distances. The GTS distances are parametrized by two parameters. A parameter w controls the weight of misclassification occurring from the uncertainty of the true labels, while a parameter σ controls by how much activities may be shifted.

Definition 2.1 (Globally Time-Shifted distance). Given $w \geq 0, \sigma > 0$ and a metric d on \mathcal{S} we define a Globally Time-Shifted distance as:

$$GTS_{w,\sigma}(f, g) = \inf_{\epsilon \in [-\sigma, \sigma]} \{\text{dist}(f \circ \tau_\epsilon, g) + w|\epsilon|\},$$

where for $\epsilon > 0$ $\tau_\epsilon : \mathbb{R} \rightarrow \mathbb{R}$ is a time shift defined as follows:

$$\tau_\epsilon(t) = t - \epsilon.$$

A GTS distance is defined for $f, g \in \mathcal{T}$ and it is possible that the distance is infinite.

Depending on the choice of parameters the GTS distance possesses certain properties. For $w > 0$ and $\sigma = \infty$, the GTS distance is an extended metric² and a proof of this fact is given in the appendix. If $w > 0$ and $\sigma > 0$, then it

²It may attain the value ∞ .

is a semimetric meaning that it has all properties required for a metric, except for the triangle inequality. Indeed, consider the following example. Let f, g, h be functions defined by

$$f = \mathbb{1}_{[0.2,0.8)}, g = \mathbb{1}_{[0.4,1)}, h = \mathbb{1}_{[0.3,0.9)}.$$

Let d be the discrete metric on $S = \{0, 1\}$, $\sigma = 0.1$ and $w = 0.6$. In this case we have

$$\begin{aligned} GTS_{w,\sigma}(f, g) &= 0.26, \\ GTS_{w,\sigma}(f, h) + GTS_{w,\sigma}(h, g) &= 0.12, \end{aligned}$$

and we see that the triangle inequality does not hold.

The main downside of the use of the GTS distance is the unrealistic assumption on timing uncertainty. However, if we know that the ground truth labels preserve the true state durations then it is a good choice. Consider a function $f \in \mathcal{T}$ with two state transitions j_1 and j_2 . Let estimate $g \in \mathcal{T}$ also feature two state transitions $j_1 - \tau_1$ and $j_2 - \tau_2$. If $\tau_1 \neq \tau_2$ have opposite signs, then there is no global time shift that can align the functions f and g . This implies that the true state durations need to be preserved in the estimate in order to align functions using the global time shift.

2.3 Locally Time-Shifted distance and the Duration Penalty Term

The global time shift stresses the state durations, which is not always desirable. For instance, if the true labels do not preserve the real state durations, or e.g. if the additive noise terms in the locations of the jumps are independent. Here is an example: figure 2 shows f and its approximations g_i for $i = 1, 2, 3$. It is impossible to align f with any of the g_i with a single time shift, however, it would be possible if each state transition could be shifted ‘locally’.

Additionally, the GTS distance is sensible only when there is at most one event in the time series, which limits its use. Naturally, to accommodate for both of these issues a suitable modification would be to replace one global time shift with multiple local time shifts. We will introduce a measure of closeness between trajectories which conceptually can be seen as derived from the GTS measure. Our approach can be compared to the one introduced in [31]. There the authors measure performance based on segments, which are intervals in which neither the ground truth labels nor the estimate change the state. If the state in the estimate and the state in the ground truth labels agree in a given segment, we can classify it as correctly classified. If that were not true, the authors provide a variety of different classifications of segments, such as fragmenting segment or inserted segment. This provides a deeper level of error characterization, which is then used in different metrics of classifier performance.

In our case, the characterization will be focused on whether the error is caused by the timing uncertainty or some other cause. We will be working with

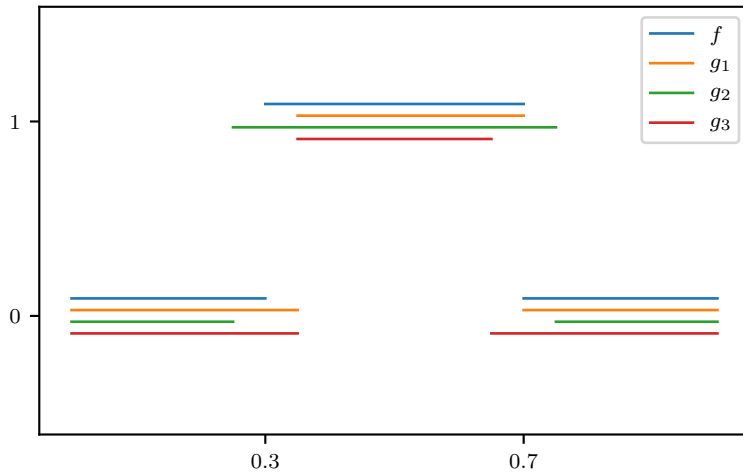


Figure 2: The function f represents the ground truth labels with an uncertainty around state boundaries, g_i are the approximations of f .

sequences of jumps, but more specifically given two sequences of state boundaries we will combine them together and sort the resulting joint sequence in an increasing order. Subsequent pairs of values in this sequence are determining segments understood as in [31]. We weigh different types of segments and the result is a weighted average of segment lengths, which is supposed to reflect well the error magnitude of the classifier.

We define segments formally and introduce a new distance on \mathcal{T} .

Definition 2.2 (Segments). Let $f, g \in \mathcal{T}$. The elements of the smallest partition³ of \mathbb{R} such that in each element of the partition neither f nor g changes state will be called segments.

Since functions from \mathcal{T} are piece-wise constant and have a finite number of discontinuities, there is always a finite number of segments. The general form of segments that we will use is as follows:

$$(-\infty, a_1) \cup \bigcup_{i=1}^{l-1} [a_i, a_{i+1}) \cup [a_l, \infty), \quad (2)$$

where $a_1 < a_2 \dots < a_l$ if f and g are not equal everywhere. Otherwise there is only one segment, consisting of the whole real line. By convention, $a_0 = -\infty$ and $a_{l+1} = \infty$, and

$$f(a_0) = f(a_1^-) = \lim_{x \rightarrow -\infty} f(x), \quad f(a_{l+1}) = f(a_l).$$

³A partition that cannot be made coarser

Similarly to the GTS distance, parameter w controls the weight of misclassification occurring from the uncertainty of the true labels. The case when $w < 1$ is more interesting to us, since then we assume timing uncertainty of labels.

Definition 2.3 (Locally Time-Shifted distance). Let $w \geq 0$, $\sigma > 0$ and d be a metric on \mathcal{S} . Let $f, g \in \mathcal{T}$ and their set of segments to be denoted as in (2). We define the Locally Time-Shifted distance (LTS distance) as

$$LTS_{w,\sigma}(f, g) = \sum_{i=1}^{l-1} \delta_i(a_{i+1} - a_i) d(f(a_i), g(a_i)),$$

where

$$\delta_i = \begin{cases} w, & a_{i+1} - a_i \leq \sigma, f(a_{i-1}) = g(a_{i-1}), f(a_{i+1}) = \\ & g(a_{i+1}) \\ 1, & \text{otherwise.} \end{cases}$$

If $f(a_l) \neq g(a_l)$, then $LTS_{w,\sigma}(f, g) = \infty$ and if there is only one segment (functions are equal on the whole real line), then $LTS_{w,\sigma}(f, g) = 0$.

The LTS distance is an extended semimetric for $w > 0$ (proof in the appendix). The triangle inequality does not hold in general. Let f, g, h be functions defined by

$$f = \mathbb{1}_{[0,+\infty)}, g = \mathbb{1}_{[\sigma,+\infty)}, h = \mathbb{1}_{[2\sigma,+\infty)}.$$

We have $LTS_{w,\sigma}(f, h) = 2\sigma \cdot d(0, 1)$, $LTS_{w,\sigma}(f, g) = LTS_{w,\sigma}(g, h) = w\sigma \cdot d(0, 1)$. Hence for $w < 1$, $LTS_{w,\sigma}(f, h) > LTS_{w,\sigma}(f, g) + LTS_{w,\sigma}(g, h)$.

The LTS distance itself addresses the issue of timing uncertainty in the true labels. The issue that some states in the state sequence are too short still remains. Let $\gamma > 0$ be the lower bound on the durations of the states as determined by the domain knowledge (or through estimation if possible). Let $\lambda > 0$ be the penalty for each violation of the lower bound condition. For $f \in \mathcal{T}$ with its discontinuities j_1, \dots, j_n , we introduce a *duration penalty term*:

$$DP_{\lambda,\gamma}(f) = \lambda \sum_{k=1}^{n-1} \mathbb{1}_{\{x:x<\gamma\}}(j_{k+1} - j_k).$$

This term will allow to lower the performance of classifications with unrealistically short states.

In practice, we will need to extend the functions to the real line in order to use the LTS distance as its definition applies only to functions defined on whole of \mathbb{R} . Hence, an extension is necessary. One natural extension could be to extend the first and the last state of each function indefinitely. However, this solution leads to a problem. Consider two functions f and g that differ only on the interval $[0, A)$. No matter how small A is, the distance between f and g will always be infinite when using this extension, since in this case f

and g are in different states on the whole half line $(-\infty, A)$. Both functions need to be extended by the same state for the distance to be finite. We extend any function f defined on interval $[0, T]$ to the real line, setting its value to an arbitrary state s_1 outside of $[0, T]$:

$$f^*(t) = \begin{cases} f(t), & t \in [0, T] \\ s_1, & t \notin [0, T]. \end{cases} \quad (3)$$

We combine the LTS distance and the duration penalty term to define the LTS measure of closeness of two trajectories.

Definition 2.4. Let f be a function of true labels and g its estimate, both defined on $[0, T]$. The *LTS measure* is defined as:

$$LTS_{w,\sigma,\lambda,\gamma}(f, g) = \exp(-LTS_{w,\sigma}(f^*, g^*)/T - DP_{\lambda,\gamma}(g)).$$

The scaling through the division by T normalizes the LTS distance to the interval $[0, 1]$. The transformation $[0, +\infty) \ni x \rightarrow \exp(-x) \in (0, 1]$ maps the sum of the LTS distance and the duration penalty term to the interval $(0, 1]$, while reversing the order as well: g is closer to f if the LTS measure is closer to 1.

3 Improving classification by imposing physical restrictions

3.1 Post-processing by projection

When choosing a classifier for the task of activity recognition, we are often faced with a dilemma. We can choose a classifier that captures the underlying nature of the data better, for instance a classifier that assumes time dependence in the data through the semi-Markov property. Then the computational cost of estimation can be high and the estimation itself might be of lesser quality if there is not enough data or the quality of the data is poor. If we choose a simpler classifier we have no problems learning the parameters of the method, but the restrictive assumptions of a simple classifier might not be satisfied. For a simple classifier one typically assumes independence between the observations; an assumption especially dangerous in the case of activity recognition since the data coming from sensors are highly time-dependent. One way to mitigate this problem is to use the sliding window technique that equips each time point with some knowledge about the past and the future, however, simple classifiers (such as decision trees) themselves are not capable of using the information about the distribution of durations in their prediction. The goal of this section is to provide a post-processing procedure that corrects for classifier’s mistakes regarding the distribution of durations.

Now we specifically focus on binary setting, so $\mathcal{S} = \{0, 1\}$ are the states.

Definition 3.1 (Function with bounded minimum duration of states). Given parameter $\gamma > 0$ we define $\mathcal{G}_\gamma \subset \mathcal{T}$, the set of functions with *bounded minimum duration of states*, such that for $g \in \mathcal{G}_\gamma$ we have

- $g = \sum_{i=1}^N \mathbb{1}_{[L_i, U_i)}$ for some constant $N \in \mathbb{N}$ and an increasing sequence $L_1 < U_1 < L_2 < \dots < U_N$ (we allow $L_1 = -\infty$ and $U_N = \infty$),
- if $N \geq 1$, then $\forall_i U_i - L_i \geq \gamma$ and $\forall_{i>1} L_i - U_{i-1} \geq \gamma$.

We will project \mathcal{T} onto \mathcal{G}_γ . As a measure of closeness between functions from \mathcal{T} and \mathcal{G}_γ , we use the standard distance on \mathcal{T} as defined in (1) (with the discrete metric d on \mathcal{S}) together with a penalization of jumps of g . In this case, the standard distance on \mathcal{T} coincides with the L_1 -distance (when $\mathcal{S} = \{0, 1\}$). Let $f \in \mathcal{T}$ and $g \in \mathcal{G}_\gamma$. Then we introduce the notation:

$$E_\gamma(f, g) = \|f - g\|_1 + \gamma \cdot J(g)/2, \quad (4)$$

where $J(g)$ is the number of jumps of g .

Given $f \in \mathcal{T}$, our goal is to find $\hat{f} \in \mathcal{G}_\gamma$ such that

$$\hat{f} = \arg \min_{g \in \mathcal{G}_\gamma} E_\gamma(f, g) \quad (5)$$

and then \hat{f} is called a projection of f onto \mathcal{G}_γ .

The regularization by penalizing high numbers of jumps narrows down the set of possible solutions to a finite nonempty subset of \mathcal{G}_γ (as will be shown later), which leads to the existence of \hat{f} . The solution might not be unique, as illustrated by the following example.

Let $f = \mathbb{1}_{[0.35, 0.45)} + \mathbb{1}_{[0.55, +\infty)}$ and $\gamma = 0.2$. Both $\hat{f}_1 = \mathbb{1}_{[0.35, +\infty)}$ as well as $\hat{f}_2 = \mathbb{1}_{[0.55, +\infty)}$ are the projections of f . One could think of it as an issue, however, it does reflect well our understanding of the original problem. The assumption is that f has impossibly short windows, because it is uncertain which activity is actually performed in the interval $[0.35, 0.55)$. Looking only at f we are unable to decide ourselves which solution is more suitable, hence it is only natural that the method also returns two possible options. Nevertheless, in real applications we can expect that such a situation will occur rarely.

3.2 Connection with the shortest path problem

In general, finding \hat{f} might not be an easy task. As an example, consider figure 3, where the function f was projected onto $\mathcal{G}_{0.5}$. Checking all possible functions from $\mathcal{G}_{0.5}$ is naturally infeasible, but also there does not seem to be any clear rule with regards to which jumps should be present in a projection. Naively, we could think that the shorter segments are removed and in general we can see this is somewhat true, but a good counterexample to this rule are the short activities in the interval $[8, 9]$.

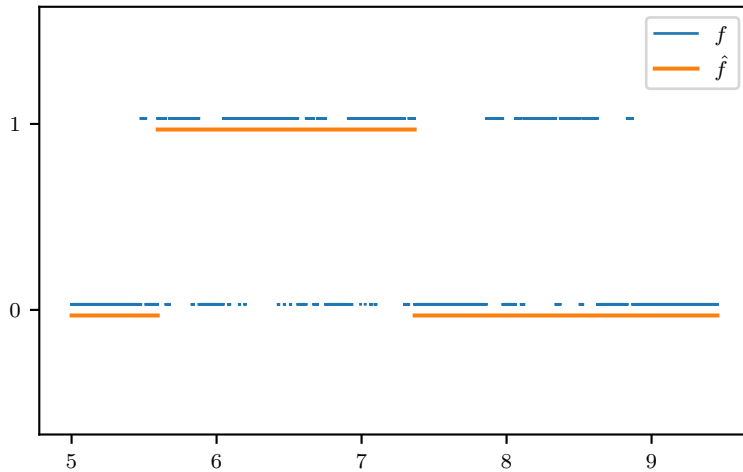


Figure 3: Example of projecting function from \mathcal{T} onto $\mathcal{G}_{0.5}$

We will devise a method for finding a projection in an efficient manner. A function f can have multiple uninterrupted intervals shorter than γ . Each sequence of these intervals can be studied separately in order to find the optimal \hat{f} as proved in the appendix. It is implied from the proof that a projection will not introduce new jump locations since in that case the L_1 -penalty could always be reduced by moving the new jump locations to jump locations of the original function. Without loss of generality we will assume that f has $n \geq 2$ jumps at time points j_i for $i = 1, \dots, n$, such that $0 < j_i - j_{i-1} < \gamma$ for $i = 2, \dots, n$, and no other jumps are made. Since we can always consider the function $1 - f$ instead of f , we will also assume that f takes value 0 in the interval $(-\infty, j_1)$. Lastly, we use the following notation: $j_0 = -\infty$, $j_{n+1} = \infty$.

Now we introduce the problem of finding the shortest path in a graph, which is equivalent to finding \hat{f} as will be shown later. We will now define the graph for the shortest path problem. Let $G = (V, A)$ be a directed graph such that the set of vertices V is given by

$$V = \{j_0, j_1, \dots, j_n, j_{n+1}\} \setminus \{j_2, j_{n-1}\} \quad (6)$$

and the set of directed arcs is given by

$$A = \left(\bigcup_{l=0}^n A_l \right) \setminus \{A_2\}, \quad (7)$$

where:

$$\begin{aligned}
A_0 &= \{(j_0, j_k) : \forall_{k \in \{1, \dots, n+1\} \setminus \{n-1\}} \quad k \bmod 2 = 1\}, \\
A_l &= \{(j_l, j_k) : \forall_{k \in \{l+3, \dots, n+1\} \setminus \{n-1\}} \quad k - l \equiv 1 \pmod{2}\}, \\
l &= 1, \dots, n-2, \\
A_{n-1} &= \emptyset, \\
A_n &= \{(j_n, j_{n+1})\}.
\end{aligned}$$

There is a correspondence between each path from j_0 to j_{n+1} and a sequence of jumps in the interval $(j_1 - \gamma, j_n + \gamma)$. A path $(j_0, j_{l_1}, \dots, j_{l_m}, j_{n+1})$ represents a function g with jumps at j_{l_1}, \dots, j_{l_m} , such that $f(j_{l_k}) = g(j_{l_k})$. As we can see some jumps of f are not present in V and many of the possible arcs are excluded from A as well. It is shown later that such V and A are sufficient to find an optimal \hat{f} . However, not all paths correspond to a function from \mathcal{G}_γ . We will introduce a weight function $w : A \rightarrow \mathbb{R}_+$ ensuring that every path of finite cost corresponds to a function from \mathcal{G}_γ and, moreover, that the cost of the path coincides with the error $E(f, \cdot)$ of the corresponding function in the interval $(j_1 - \gamma, j_n + \gamma)$. Let $I_k = j_{k+1} - j_k$ for $k = 0, \dots, n$. It is noteworthy that $I_0, I_n = \infty$, while $I_k < \gamma$ for $k = 1, \dots, n-1$. We introduce penalty for a jump $J_k = \gamma/2$ for $k = 1, \dots, n$ and $J_{n+1} = 0$. The function $H_\gamma : \mathbb{R} \rightarrow \overline{\mathbb{R}}$, validating the assumption of the class \mathcal{G}_γ , is defined as follows:

$$H_\gamma(x) = \begin{cases} \infty, & x < \gamma \\ 0, & x \geq \gamma. \end{cases}$$

Now we define the weight function w :

$$w((j_k, j_l)) = H_\gamma(j_l - j_k) + \sum_{\substack{m=k+1 \\ m \equiv k+1 \pmod{2}}}^{l-2} I_m + J_l, \quad (8)$$

for all possible arcs (j_k, j_l) , where by convention $\sum_{m=a}^b c_m = 0$ for all $a > b$. The first term in this formula ensures that $[j_k, j_l]$ is an interval longer than or equal to γ . The second term finds the L_1 norm of $f - g$ in $[j_k, j_l]$. The last term adds a penalty for jump at j_l if j_l is finite (the penalty for jump at j_k was added on a previous arc in the path, if $k > 0$).

Lemma 3.1. *Let $\gamma > 0$ and $f \in \mathcal{T}$. Let J denote the set of all discontinuities of the function f . If a function $g \in \mathcal{G}_\gamma$ contains jumps outside of J or jumps from J , but in an opposite direction than in f , g cannot be a projection of f onto \mathcal{G}_γ .*

Theorem 3.1 (Problem equivalence). *Let $\gamma > 0$ and (j_1, \dots, j_n) be the only discontinuities of a function $f \in \mathcal{T}$. Let $G = (V, A, w)$ be a weighted, directed graph defined as in (6), (7), (8) above. The task of finding a projection of f onto \mathcal{G}_γ , defined as in (5), is equivalent to finding the shortest path from j_0 to j_{n+1} in the graph G .*

The proof of the lemma and the theorem can be found in the appendix. As pointed out in the proof, it is important that the weight of the jump penalty in E is at least $\gamma/2$. On the other hand the weight can be at most $\gamma/2$, in order to study each uninterrupted sequence of intervals shorter than γ separately. This motivates our choice for $\gamma/2$ as the weight. Now, we will illustrate the method by an example.

Given $\gamma = 0.2$, consider the function $f = \mathbb{1}_{[0.2,0.35]} + \mathbb{1}_{[0.4,0.55]}$ and all its possible projections: $g_1 \equiv 0$, $g_2 = \mathbb{1}_{[0.2,0.55]}$, $g_3 = \mathbb{1}_{[0.35,0.55]}$, $g_4 = \mathbb{1}_{[0.2,0.4]}$. We can calculate the closeness of each g_i from f :

$$\begin{aligned} E(f, g_1) &= 0.3, & E(f, g_2) &= 0.25, \\ E(f, g_3) &= 0.4, & E(f, g_4) &= 0.4 \end{aligned}$$

and conclude that g_2 is the projection of f onto $\mathcal{G}_{0.2}$.

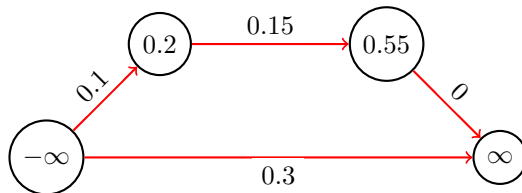


Figure 4: Graph G constructed for the function f .

We will construct the graph G , defined as in (6), (7), (8), for f . The sets of vertices and arcs are as follows

$$\begin{aligned} V &= \{-\infty, 0.2, 0.55, \infty\}, \\ A &= \{(-\infty, 0.2), (-\infty, \infty), (0.2, 0.55), (0.55, \infty)\} \end{aligned}$$

and the weights are shown in figure 4. There are two possible paths from $-\infty$ to ∞ . The path $P_1 = (-\infty, 0.2, 0.55, \infty)$ has the cost equal to 0.25, while the path $P_2 = (-\infty, \infty)$ has the cost 0.3. Since P_1 has a lower cost, we conclude again that g_2 is the projection of f onto $\mathcal{G}_{0.2}$.

In general, we can use the following known algorithm (exercise 22.4-2 in [33, pp. 614]) to find the shortest path between j_0 and j_{n+1} . Let G be any directed acyclic graph (DAG), w the corresponding weight function, s the source and e the end.

The total running time of the algorithm is $\Theta(|V| + |A|)$. It is also worth noting that in our case V is already topologically sorted. Figure 5 shows the linearity of the running time as a function of $|V| + |A|$ and figure 6 shows the graph size as a function of number of jumps. It is worth noting that in application of the real data we did not encounter sequences of jumps of length greater than 400.

Algorithm 1 Finding shortest path in directed acyclic graph

```
1: procedure DAG-SHORTESTPATHS( $G, w, s, e$ )
2:   topological sort of graph  $G$ 
3:   for  $v \in V$  do
4:      $v.d = \infty$  // cost of the currently shortest distance from  $s$  to  $v$ 
5:      $v.\pi = \text{NULL}$  // predecessor of  $v$  on the currently shortest path
6:    $s.d = 0$ 
7:   for  $u \in V$ , taken in topologically sorted order do
8:     for each neighbour  $v$  of vertex  $u$  do
9:       if  $v.d > u.d + w((u, v))$  then
10:         $v.d = u.d + w((u, v))$ 
11:         $v.\pi = u$ 
12:    $\text{shortestPath} \leftarrow$  empty array
13:    $\text{currNode} \leftarrow e$ 
14:   while  $\text{currNode} \neq s$  do
15:     append  $\text{currNode}$  to  $\text{shortestPath}$ 
16:      $\text{currNode} \leftarrow \text{currNode}.\pi$ 
17:   append  $s$  to  $\text{shortestPath}$ 
18:   reverse  $\text{shortestPath}$ 
19:   return  $\text{shortestPath}, e.d$ 
```

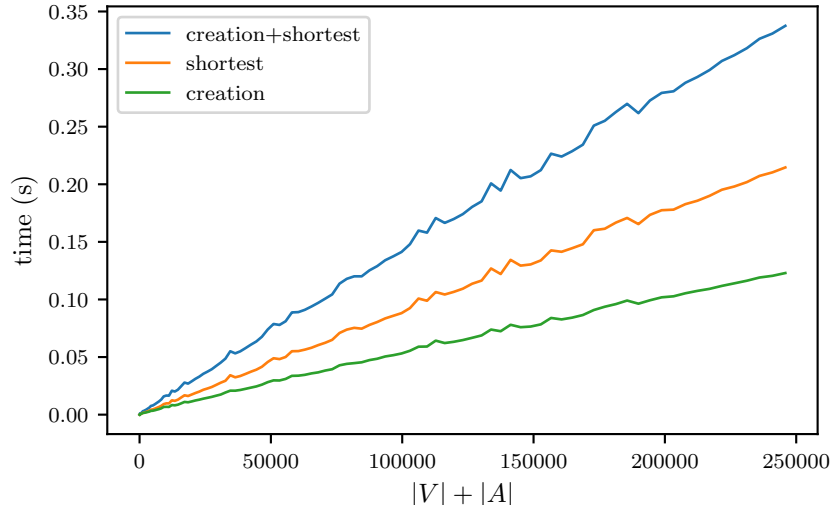


Figure 5: Running time of the algorithm 1 as a function of $|V| + |A|$

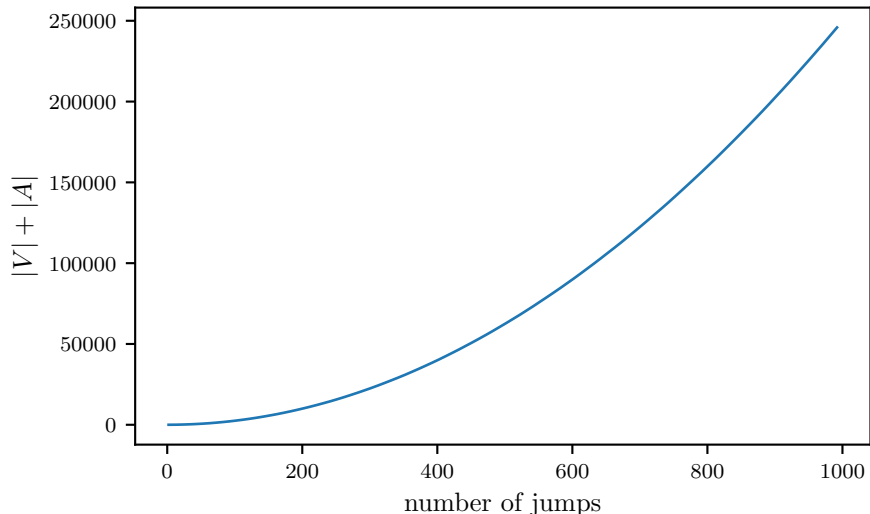


Figure 6: Graph size as a function of number of jumps

4 Application to activity recognition in football

We will now demonstrate the benefits of the post-processing by projection, utilizing the LTS measure to compare different methods of classification. First, we will describe the dataset further. Recall that the data comes from IMU sensors located on 5 different body parts: left shank (LS), right shank (RS), left thigh (LT), right thigh (RT) and pelvis (P). Each IMU sensor contains a 3-axis accelerometer (Acc) and a 3-axis gyroscope (Gyro). The naming convention will be as follows: LSAccX refers to the x -axis of the accelerometer located on the left shank. The data come in the form of short time series, each containing one exercise only. The type of the exercise is always given, but it is possible for the time series to contain other activities as well, such as standing. To show the advantages of post-processing by projection, we select only two states: standing and another activity encoded as 0 and 1, respectively. 15 time series (representative of all possible actions performed by athletes) were manually labelled time point by time point in order to be able to train classifiers, and these will form our sample.

In pre-processing we are using the sliding window technique on the sensors [34]. This method transforms the original raw data using windows of fixed length d and a statistic of choice T : given a time point t , its neighbourhood of size d is fed to the statistic T for each variable separately. Performing the procedure for each time point results in a time series of the same dimension as the original one, but every observation is equipped with some knowledge

about the past and the future through the statistic T and through forming the neighbourhoods of size d . Regarding the choice of statistic T one needs to be careful, since the sensors are highly correlated with each other. The information about standing contained in one variable is comparable to the one in another, namely the variance of the signal is low when the person is standing (differences can occur when considering different legs; a low variance on one leg might be misleading since the other leg might already be transitioning into another state).

10-fold cross-validation will be performed in order to select the best performing classification method. 10 time series will be used for training and 5 for testing. A typical approach to k -fold cross-validation with a training sample of size $k - 1$ cannot be applied here, since a single time series is not a representative sample of different types of events. The results are going to be shown for post-processed classifiers, unless specified otherwise. Before cross-validation can be performed, we need to fix the parameters of the performance measure we introduced in section 2. The parameters of the LTS measure are chosen as follows:

- We have limited information regarding how uncertain locations of state transitions are, but based on the small experiment described in section 2.1 we select $\sigma = 0.35$ (the largest deviation between different ground truth labels).
- A weight w of the time shift represents the importance (or the certainty) of state transitions in the ground truth. It will be selected as follows. We know that the visualization tool applied for manual labelling used 0.1s as the smallest step. Additionally in our problem it is difficult to find transitions between states objectively, hence we can expect state transitions to be misplaced on top of the limitations of the tool used for labelling. An experiment in section 2.1 regarding timing uncertainty in the ground truth labels shows that the standard deviation of state transitions placement ranges from 0.09s to 0.34s (we keep in mind that the sample size was very small). It seems that for some activities it is more difficult to identify the boundaries than for others. Hence, we allow for additional 0.05s on top of the limitation of the visualization tool. If $w = 0.6$, then the maximum time shift $\sigma = 0.35$ is lowered by almost 0.15s in error measurement, hence we select 0.6 as w .
- The lower bound γ on the duration of activities is selected as the length of the shortest activity in the learning dataset, which is equal to 0.8s in our case.
- A penalty λ represents the cost of additional or missing jumps in a state sequence compared to the ground truth labels. Since an estimate already pays an L_1 penalty for misclassification, the penalty λ should only be supplementary. We decide for the penalty $\lambda = 0.01$ s. It is important that the penalty λ is positive as illustrated in figure 7. Both estimates are equal in performance without the penalization by λ , but with it estimate 1 is performing better.

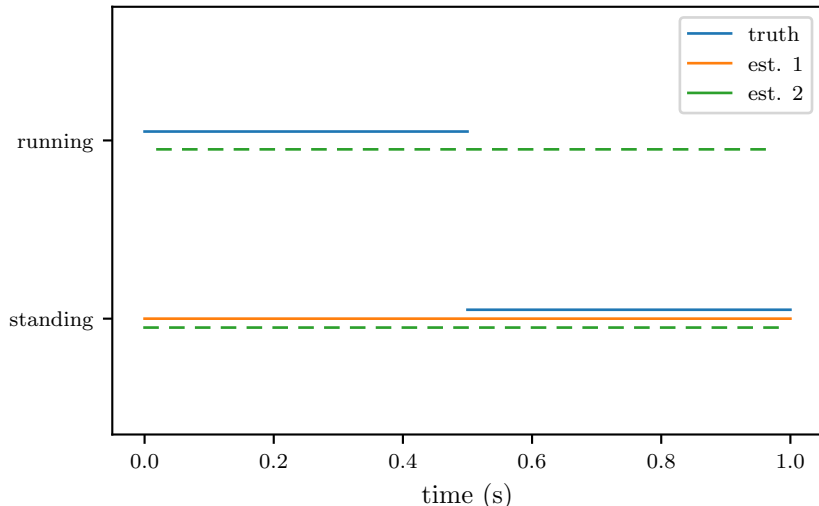


Figure 7: An importance of including penalty for violating the lower bound on the duration of activities.

Before assessing classifiers on the training set, one needs to consider an appropriate feature set. Our variables are highly dependent on one another, so we start with feature selection. The setup is two-fold: first we perform feature ranking using the Relief algorithm [35]. The algorithm is iterative; weights of the features are initialized to zeroes and R observations are randomly drawn from the training sample. For each observation r_i we find its k nearest hits H_i (samples with the same state as the drawn observation) and k nearest misses M_i (samples with a different state than the drawn observation) in the feature space with Euclidean distance. The weight of a feature a is updated as follows:

$$w(a) = w(a) + \sum_{i=1}^R \left(\sum_{h \in H_i} |h(a) - r_i(a)| - \sum_{m \in M_i} |m(a) - r_i(a)| \right).$$

In the next step we choose the 6 most relevant features based on the Relief weights (6 features out of 30, results in 80% reduction of the feature set). Then we test all possible combinations of these features, which is now computationally feasible, in order to find the best set for each of the classifiers. The features selected by the Relief algorithm are RTGyroX, RTGyroY, RTAccX, RTAccZ, LTAccY, PAccY.

Proceeding with the cross-validation we select the following classifiers (with their abbreviations) to be assessed: DT - Decision Tree, kNN - k-Nearest Neighbors, LR - Logistic Regression, MLP - Multi-layer Perceptron, NB - Naive Bayes, RF - Random Forest, SVM - Support Vector Machine. The results of 10-fold cross-validation are shown in table 2. It is striking that all classifiers are on

Classifier	OG Test	PP Test
MLP	0.916+/-0.031	0.972+/-0.008
LR	0.898+/-0.034	0.968+/-0.015
kNN	0.59+/-0.05	0.967+/-0.020
RF	0.83+/-0.07	0.966+/-0.017
SVC	0.894+/-0.034	0.966+/-0.017
DT	0.83+/-0.07	0.965+/-0.008
NB	0.88+/-0.04	0.944+/-0.023

Table 2: Average of the 10-fold cross-validation scores for all classifiers using the best sensor set for each of them. The pre-processing consisted of the sliding window technique in combination with summarizing by the standard deviation. The OG Test averages the LTS measure on the test set for the original classifier, while the PP Test is the same value for the post-processed classifier.

average within 2.8% of test score. This is due to post-processing by projection. The correction it provides brings all classifiers closer together. This astonishing result can be extended even further. The test score of a decision tree ranges from 59% to 86% for different sensor sets before post-processing, while using the post-processing results in a range of test scores from 93% to 96.5% and this is not specific to decision trees only.

The example shows that the post-processing is crucial. First, it increases accuracy of a given estimator on a given feature set by 35%. Second, it diminishes the impact of feature selection as the difference in accuracy between different feature subsets decreases substantially. Feature selection is of course still important as it decreases computational complexity of the problem and allows to get rid of redundancy in the feature set. However, with methods that only rank features such as Relief the choice of the threshold we choose to classify a feature as significant or not is less important. Finally and most importantly, the post-processing by projection allows to select a method according to criteria other than the performance, namely the computational speed.

5 Conclusion

This paper introduces measures of classifier performance in the task of activity recognition using wearable sensors. It addresses the issue of timing offsets as well as unrealistic classifications, while retaining a typical scalar output of a performance measure allowing for easy comparisons between classifiers.

We have also introduced a post-processing scheme that allows to improve estimates in the binary setting. It finds estimated activities that are too short and eliminates them in an optimal way by finding the shortest path in a directed acyclic graph.

Real-life football sensor data were used to assess the adequacy of the post-

processing scheme. It significantly improved performance of the classifiers. At the same time, post-processed classifiers are closer to each other in performance than the original ones. This allows placing more importance on other criteria, such as the computational speed of a method.

Acknowledgments

We thank Erik Wilmes for providing football data of high quality and the stick-model animation tool. It was the basis for the analysis of our methods in section 4. We also thank Bart van Ginkel for the idea of how to generalize from the binary to the multiclass case. This work is part of the research programme CAS with project number P16-28 project 2, which is (partly) financed by the Dutch Research Council (NWO).



A Proofs

GTS distance with $w > 0$ and $s = \infty$ is an extended metric

Proof. We will show that:

$$GTS_w(f, g) = \inf_{\epsilon \in \mathbb{R}} \{\text{dist}(f \circ \tau_\epsilon, g) + w|\epsilon|\}$$

is an extended metric on \mathcal{T} .

0. Since for any ϵ , $\text{dist}(f \circ \tau_\epsilon, g) \geq 0$ and $w|\epsilon| \geq 0$ we conclude that the GTS_w is non-negative.
1. It is obvious to see that $GTS_w(f, f) = 0$ for any $f \in \mathcal{T}$. Now let us assume that for some $f, g \in \mathcal{T}$ we have $GTS_w(f, g) = 0$. This implies that

$$\exists_{(\epsilon_n)} \text{dist}(f \circ \tau_{\epsilon_n}, g) + w|\epsilon_n| \xrightarrow{n \rightarrow \infty} 0.$$

Since $\text{dist}(f \circ \tau_\epsilon, g) + w|\epsilon|$ is an upper bound of $\{\text{dist}(f \circ \tau_\epsilon, g), w|\epsilon|\}$, we have

$$\begin{aligned} |\epsilon_n| &\xrightarrow{n \rightarrow \infty} 0, \\ \int_{\mathbb{R}} d(f \circ \tau_{\epsilon_n}(t), g(t)) d\lambda(t) &\xrightarrow{n \rightarrow \infty} 0. \end{aligned}$$

From Fatou's lemma we have

$$\int_{\mathbb{R}} \liminf_{n \rightarrow \infty} d(f(t - \epsilon_n), g(t)) d\lambda(t) = 0,$$

where λ is the Lebesgue measure on \mathbb{R} . Because f and g are càdlàg and d is continuous, this implies that for almost all t we have $f(t-) = g(t)$ or $f(t) = g(t)$ and so we conclude that $f = g$ almost everywhere.

2. Let $f, g \in \mathcal{T}$, we have following

$$\begin{aligned} GTS_w(f, g) &= \inf_{\epsilon} \{\text{dist}(f \circ \tau_\epsilon, g) + w|\epsilon|\} = \inf_{\epsilon} \{\text{dist}(g \circ \tau_{-\epsilon}, f) + w|-\epsilon|\} \\ &= \inf_{-\epsilon} \{\text{dist}(g \circ \tau_\epsilon, f) + w|\epsilon|\} = \inf_{\epsilon} \{\text{dist}(g \circ \tau_\epsilon, f) + w|\epsilon|\} \\ &= GTS_w(g, f), \end{aligned}$$

hence we conclude that GTS_w is symmetric.

3. Letting $f, g, h \in \mathcal{T}$, we have following

$$\begin{aligned}
GTS_w(f, g) &= \inf_{\epsilon} \{ \text{dist}(f \circ \tau_{\epsilon}, g) + w|\epsilon| \} \\
&= \inf_{\epsilon_1, \epsilon_2} \{ \text{dist}(f \circ \tau_{\epsilon_1} \circ \tau_{\epsilon_2}, g) + w|\epsilon_1 + \epsilon_2| \} \\
&\leq \inf_{\epsilon_1, \epsilon_2} \{ \text{dist}(f \circ \tau_{\epsilon_1} \circ \tau_{\epsilon_2}, h \circ \tau_{\epsilon_2}) + \text{dist}(h \circ \tau_{\epsilon_2}, g) + \\
&\quad + w|\epsilon_1| + w|\epsilon_2| \} \\
&= \inf_{\epsilon_1, \epsilon_2} \{ \text{dist}(f \circ \tau_{\epsilon_1}, h) + w|\epsilon_1| + \text{dist}(h \circ \tau_{\epsilon_2}, g) + w|\epsilon_2| \} \\
&= \inf_{\epsilon_1} \{ \text{dist}(f \circ \tau_{\epsilon_1}, h) + w|\epsilon_1| \} + \inf_{\epsilon_2} \{ \text{dist}(h \circ \tau_{\epsilon_2}, g) + w|\epsilon_2| \} \\
&= GTS_w(f, h) + GTS_w(h, g),
\end{aligned}$$

which shows that GTS_w satisfies triangle inequality and that concludes the proof. \square

The LTS distance with $w > 0$ is a semimetric

Proof. Let $w > 0, \sigma > 0$ and a metric d on \mathcal{S} be fixed. We observe that $LTS_{w, \sigma}$ is nonnegative. Symmetry of $LTS_{w, \sigma}$ follows directly from the definition. It only remains to show that $LTS_{w, \sigma}(f, g) = 0$ if and only if $f = g$ for $f, g \in \mathcal{T}$. We have

$$LTS_{w, \sigma}(f, f) = 0,$$

because there is only one segment. Assume now that $LTS_{w, \sigma}(f, g) = 0$ and $f \neq g$. In that case, there exists more than one segment.

$$\begin{aligned}
LTS_{w, \sigma}(f, g) &= \sum_{i=1}^{l-1} \delta_i(a_{i+1} - a_i) d(f(a_i), g(a_i)) = 0 \\
&\Rightarrow \forall_{i=1, 2, 3, \dots, l-1} \quad f(a_i) = g(a_i),
\end{aligned}$$

which implies that $f = g$, which contradicts the assumption. We conclude that $LTS_{w, \sigma}(f, g) = 0$ iff $f = g$, which completes the proof. \square

A projection $\mathcal{T} \rightarrow \mathcal{G}_{\gamma}, f \mapsto \hat{f}$ does not change states that last longer than γ , while if a state lasts exactly γ there exists a projection that does not change it

Proof. Let f be a function with two neighboring jumps j_1, j_2 satisfying the condition $j_2 - j_1 \geq \gamma$. Since the interval is longer than or equal to γ it satisfies the condition of the class \mathcal{G}_{γ} . If $j_2 - j_1 > \gamma$, then no matter what the values of a projection \hat{f} will be outside of the interval $(j_1, j_2]$ it will always be cheaper to match the values of f on $(j_1, j_2]$ and to take a penalty of at most $2 \cdot \gamma/2 = \gamma$ for possible jumps at the boundary of the interval than to take an L_1 -penalty of at least γ by assigning a value different from f on the interval $(j_1, j_2]$. If $j_2 - j_1 = \gamma$, then whether we match the values of f on (j_1, j_2) or remove the jumps at j_1 and j_2 we take penalty of exactly γ . There is no unique projection in this case, but one of them allows no change of the state. \square

Proof of Lemma 3.1 Let \hat{f} be a projection of f onto \mathcal{G}_γ . Assume that \hat{f} contains a jump j such that it is outside of the set J of discontinuities of f or it is inside J , but is in opposite direction than in f .⁴ Without loss of generality we assume j is a jump from 0 to 1. Amongst jumps of f closest to j from the left and from the right we denote by j_k the one from 0 to 1. Such jump exists, otherwise in the case of $j \notin J$, \hat{f} would differ from f on an infinite interval to the left or to the right of j or there would exist a state in \hat{f} not present in f , while in the case of $j \in J$, but in opposite direction than in f this would imply that f has only one jump, at j , which is false and hence \hat{f} could not have been a projection of f onto \mathcal{G}_γ . Without loss of generality we assume j_k is the jump of f closest to j from the left. Let j_a be a jump of \hat{f} preceding j (if such jump does not exist then $j_a = -\infty$). It is important to note that $j_k \geq j_a$, unless j_k is the last jump of f (which can only happen if $j \notin J$), in which case it is trivial to see that \hat{f} can be easily improved upon to reduce error (by removing jumps j_a and j entirely) which contradicts its optimality. If $j_k - j_a \geq \gamma$, then moving the jump of \hat{f} from j to j_k results in the reduction of error by $j - j_k$, which contradicts the assumption of optimality of \hat{f} . If $j_k - j_a < \gamma$, then removing jumps j_a and j from \hat{f} yields a better approximation (increase in L_1 norm is smaller than γ , while decrease in jump penalty is equal to γ). Hence \hat{f} cannot be a projection of f . \square

Proof of Theorem 3.1 We use Lemma 3.1 twice to prove that a projection of a function from \mathcal{T} onto \mathcal{G}_γ can only make jumps at the some positions and in the same directions as the jumps in the projected function. This leads to the fact that finding the shortest path in the graph defined in the paper is a problem equivalent to finding \hat{f} . \square

References

- [1] Wesllen S. Lima et al. “User activity recognition for energy saving in smart home environment”. In: *Proceedings of the 2015 IEEE Symposium on Computers and Communication (ISCC)*. New York, NY: IEEE, 2015, pp. 751–757.
- [2] Markus Eckelt, Franziska Mally, and Angelika Brunner. “Use of Acceleration Sensors in Archery”. In: *Proc.* 49 (2020), p. 98. URL: <https://doi.org/10.3390/proceedings2020049098>.
- [3] Stylianos Paraschiakos et al. “Activity recognition using wearable sensors for tracking the elderly”. In: *User Model. and User-Adapt. Interact.* 30 (2020), pp. 567–605. URL: <https://doi.org/10.1007/s11257-020-09268-2>.

⁴The proof should first be conducted for the case of a jump outside of J and then for the case of a jump in opposite direction than in f .

- [4] Oscar Martinez Mozos et al. “Stress Detection Using Wearable Physiological and Sociometric Sensors”. In: *Int. J. of Neural Syst.* 27 (2017), p. 1650041. URL: <https://doi.org/10.1142/S0129065716500416>.
- [5] Maurits Waterbolk et al. “Detection of Ships at Mooring Dolphins with Hidden Markov Models”. In: *Transp. Res. Rec.* 2673 (2019), p. 0361198119837495. URL: <https://doi.org/10.1177/0361198119837495>.
- [6] R. Varatharajan et al. “Wearable sensor devices for early detection of Alzheimer disease using dynamic time warping algorithm”. In: *Clust. Comput.* 21 (2018), pp. 681–690. URL: <https://doi.org/10.1007/s10586-017-0977-2>.
- [7] Oliver Amft et al. “Analysis of Chewing Sounds for Dietary Monitoring”. In: *Proceedings of the UbiComp 2005: Ubiquitous Computing*. Ed. by Michael Beigl et al. Vol. 3660. Lecture Notes in Computer Science. Berlin, Heidelberg: Springer, 2005, pp. 56–72.
- [8] Agata Kolakowska, Wioleta Szwoch, and Mariusz Szwoch. “A Review of Emotion Recognition Methods Based on Data Acquired via Smartphone Sensors”. In: *Sens.* 20 (2020), p. 6367. URL: <https://doi.org/10.3390/s20216367>.
- [9] Oscar D. Lara and Miguel A. Labrador. “A Survey on Human Activity Recognition using Wearable Sensors”. In: *IEEE Commun. Surv. & Tutor.* 15 (2013), pp. 1192–1209. URL: <https://doi.org/10.1109/SURV.2012.110112.00192>.
- [10] L. Minh Dang et al. “Sensor-based and vision-based human activity recognition: A comprehensive survey”. In: *Pattern Recognit.* 108 (2020), p. 107561. URL: <https://doi.org/10.1016/j.patcog.2020.107561>.
- [11] Jindong Wang et al. “Deep learning for sensor-based activity recognition: A survey”. In: *Pattern Recognit. Lett.* 119 (2019), pp. 3–11. URL: <https://doi.org/10.1016/j.patrec.2018.02.010>.
- [12] Charissa Ann Ronao and Sung-Bae Cho. “Recognizing human activities from smartphone sensors using hierarchical continuous hidden Markov models”. In: *Int. J. of Distrib. Sens. Netw.* 13 (2017), p. 1550147716683687. URL: <https://doi.org/10.1177/1550147716683687>.
- [13] Nicole A. Capela, Edward D. Lemaire, and Natalie Baddour. “Feature selection for wearable smartphone-based human activity recognition with able bodied, elderly, and stroke patients”. In: *PLoS One* 10 (2015), e0124414. URL: <https://doi.org/10.1371/journal.pone.0124414>.
- [14] Carlos Aviles-Cruz et al. “Granger-causality: An efficient single user movement recognition using a smartphone accelerometer sensor”. In: *Pattern Recognit. Lett.* 125 (2019), pp. 576–583. URL: <https://doi.org/10.1016/j.patrec.2019.06.029>.
- [15] Shuangquan Wang and Gang Zhou. “A review on radio based activity recognition”. In: *Digit. Commun. and Netw.* 1 (2015), pp. 20–29. URL: <https://doi.org/10.1016/j.dcan.2015.02.006>.

- [16] Ramona Rednic et al. “Wearable posture recognition systems: Factors affecting performance”. In: *Proceedings of 2012 IEEE-EMBS International Conference on Biomedical and Health Informatics*. New York, NY: IEEE, 2012, pp. 200–203.
- [17] Chun Zhu and Weihua Sheng. “Motion- and location-based online human daily activity recognition”. In: *Pervasive and Mob. Comput.* 7 (2011), pp. 256–269. URL: <https://doi.org/10.1016/j.pmcj.2010.11.004>.
- [18] Maria Cornacchia et al. “A Survey on Activity Detection and Classification Using Wearable Sensors”. In: *IEEE Sens. J.* 17 (2016), pp. 386–403. URL: <https://doi.org/10.1109/JSEN.2016.2628346>.
- [19] Lu Li et al. “Indirect activity recognition using a target-mounted camera”. In: *Proceedings of the 2011 4th International Congress on Image and Signal Processing*. Ed. by Peihua Qiu et al. New York, NY: IEEE, 2011, pp. 487–491.
- [20] Michael S. Ryoo and Larry Matthies. “First-Person Activity Recognition: What Are They Doing to Me?”. In: *Proceedings of the 2013 IEEE Conference on Computer Vision and Pattern Recognition*. New York, NY: IEEE, 2013, pp. 2730–2737.
- [21] Yoshihiro Watanabe et al. “Human gait estimation using a wearable camera”. In: *Proceedings of the 2011 IEEE Workshop on Applications of Computer Vision*. New York, NY: IEEE, 2011, pp. 276–281.
- [22] Kai-Tai Song and Wei-Jyun Chen. “Human activity recognition using a mobile camera”. In: *Proceedings of the 2011 8th International Conference on Ubiquitous Robots and Ambient Intelligence (URAI)*. New York, NY: IEEE, 2011, pp. 3–8.
- [23] Ivan Laptev et al. “Learning realistic human actions from movies”. In: *Proceedings of the 2008 IEEE Conference on Computer Vision and Pattern Recognition*. New York, NY: IEEE, 2008, pp. 1–8.
- [24] Yan Ke, Rahul Sukthankar, and Martial Hebert. “Efficient visual event detection using volumetric features”. In: *Proceedings of the Tenth IEEE International Conference on Computer Vision (ICCV’05)*. Vol. 1. New York, NY: IEEE, 2005, pp. 166–173.
- [25] Chen Chen, Roozbeh Jafari, and Nasser Kehtarnavaz. “UTD-MHAD: A multimodal dataset for human action recognition utilizing a depth camera and a wearable inertial sensor”. In: *Proceedings of the 2015 IEEE International Conference on Image Processing (ICIP)*. New York, NY: IEEE, 2015, pp. 168–172.
- [26] Jamie A. Ward, Paul Lukowicz, and Gerhard Tröster. “Evaluating Performance in Continuous Context Recognition Using Event-Driven Error Characterisation”. In: *Location- and Context-Awareness*. Ed. by Mike Hazas, John Krumm, and Thomas Strang. Berlin, Heidelberg: Springer, 2006, pp. 239–255.

- [27] Chin-Chia Michael Yeh, Nickolas Kavantzias, and Eamonn Keogh. “Matrix Profile IV: Using Weakly Labeled Time Series to Predict Outcomes”. In: *Proceedings of the VLDB Endowment*. Ed. by Peter Boncz and Ken Salem. Vol. 10. VLDB Endowment, 2017, pp. 1802–1812.
- [28] Erik Wilmes et al. “Inertial Sensor-Based Motion Tracking in Football with Movement Intensity Quantification”. In: *Sens.* 20 (2020), p. 2527. URL: <https://doi.org/10.3390/s20092527>.
- [29] Wesllen Sousa Lima et al. “Human Activity Recognition Using Inertial Sensors in a Smartphone: An Overview”. In: *Sens.* 19 (2019), p. 3213. URL: <https://doi.org/10.3390/s19143213>.
- [30] Joan Serrà and Josep Lluís Arcos. “An empirical evaluation of similarity measures for time series classification”. In: *Knowl.-Based Syst.* 67 (2014), pp. 305–314. URL: <https://doi.org/10.1016/j.knosys.2014.04.035>.
- [31] Jamie A. Ward, Paul Lukowicz, and Hans W. Gellersen. “Performance Metrics for Activity Recognition”. In: *ACM Trans. on Intell. Syst. and Technol.* 2 (2011), p. 6. URL: <https://doi.org/10.1145/1889681.1889687>.
- [32] Patrick Billingsley. *Convergence of Probability Measures*. second. Hoboken, NJ: John Wiley & Sons, Inc., 1999.
- [33] Thomas H. Cormen et al. *Introduction to Algorithms*. third. Cambridge, MA: The MIT Press, 2009.
- [34] Thomas G. Dietterich. “Machine Learning for Sequential Data: A Review”. In: *Structural, Syntactic, and Statistical Pattern Recognition*. Ed. by Terry Caelli et al. Vol. 2396. Lecture Notes in Computer Science. Berlin, Heidelberg: Springer, 2002, pp. 15–30.
- [35] Igor Kononenko, Edvard Šimec, and Marko Robnik-Šikonja. “Overcoming the Myopia of Inductive Learning Algorithms with RELIEFF”. In: *Appl. Intell.* 7 (1997), pp. 39–55. URL: <https://doi.org/10.1023/A:1008280620621>.